

Kinetics and mechanisms of the elimination of ethyl and *tert*-butyl esters of carbazic acid in the gas phase: experimental and theoretical studies

Alexandra Rotinov,¹ Rosa M. Domínguez,¹ Tania Córdova² and Gabriel Chuchani^{1*}

¹Centro de Química, Instituto Venezolano de Investigaciones Científicas (IVIC), Apartado 21827, Caracas 1020-A, Venezuela

²Laboratorio de Físico-Química Orgánica, Escuela de Química, Facultad de Ciencias, Universidad Central de Venezuela, Apartado 1020-A, Caracas, Venezuela

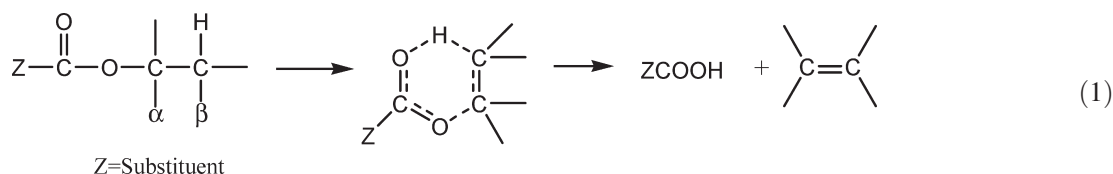
Received 18 October 2004; revised 20 December 2004; accepted 4 January 2005

ABSTRACT: The kinetics of the gas-phase elimination of ethyl and *tert*-butyl carbazates were studied in a static system over the temperature range 220.3–341.7 °C and pressure range 21.1–70.0 Torr (1 Torr = 133.3 Pa). The reactions in seasoned vessels are homogeneous, unimolecular and obey a first-order rate law. The variation of the rate coefficients with temperature is given by the following Arrhenius equations: for ethyl carbazate $\log[k_1(\text{s}^{-1})] = (11.84 \pm 0.22) - [(176.2 \pm 2.5) \text{ kJ mol}^{-1}]/(2.303 RT)^{-1}$ and for *tert*-butyl carbazate $\log[k_1(\text{s}^{-1})] = (12.34 \pm 0.29) - [(153.6 \pm 2.9) \text{ kJ mol}^{-1}]/(2.303 RT)^{-1}$. The theoretical examination indicates that the molecular mechanism corresponds to a concerted non-synchronous reaction giving the products. Bond order analysis and natural charges imply that polarization of the O(alkyl)–C(alkyl) bond of the ester is rate determining in these reactions. The rate coefficients from the experiments are in good agreement with the theoretical calculations. The mechanisms of these reactions and the role of the hydrazo group at the acid side of the ester are discussed. Copyright © 2005 John Wiley & Sons, Ltd.

KEYWORDS: kinetics; unimolecular elimination; pyrolysis; ethyl carbazate; *tert*-butyl carbazate; *ab initio* calculations; transition-state structure

INTRODUCTION

The gas-phase elimination of esters of organic acids proceed through a six-membered cyclic transition state type of mechanism as described in reaction (1). For molecular elimination, the presence of a C_β–H bond at the alkyl side of the ester is necessary.



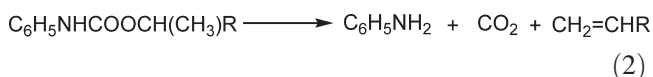
According to the general elimination reaction of esters, Herize *et al.*¹ examined the kinetic parameters for the comparative rates of different substituents other than carbon at the acid side of organic ethyl esters. These organic esters gave a good Taft–Topsom correlation¹ as described in Scheme 1.

The parameter $\sigma_{\text{F}^-} = +2.57$ suggested the field or electronic effect to be the most important influence in the elimination process. Moreover, the resonance effect

$\sigma_{\text{R}^-} = -1.18$ implied the interaction of the substituent with an incipient negative reaction center and the abstraction of the β -hydrogen of the ethyl ester by the oxygen carbonyl. The polarizability or steric effect $\sigma_{\alpha} = -0.68$ was believed to have a modest participation.

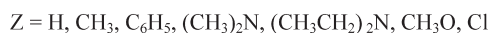
The presence of at least an H atom at the N in carbamates has been found to give a different mechanistic

pathway and product formation, as reported previously² [reaction (2)]. To avoid this type of elimination process, most studies of the pyrolytic decomposition of carbamates have been carried out with the H of the amino substituent replaced by a methyl or phenyl groups.^{3–8}



A substituent of interest to examine at the acid side of an organic ethyl ester is the hydrazo group (NH₂NH), i.e. ethyl carbazate, and possibly include it in the above

*Correspondence to: G. Chuchani, Centro de Química, Instituto Venezolano de Investigaciones Científicas (IVIC), Apartado 21827, Caracas 1020-A, Venezuela.
E-mail: chuchani@quimica.ivic.ve



$$\log k/k_0 = -(0.68 \pm 0.12)\sigma_\alpha + (2.57 \pm 0.12)\sigma_\beta - (1.18 \pm 0.27)\sigma_\beta^- (r = 0.984, \text{sd} = 0.119 \text{ at } 400^\circ\text{C})$$

Scheme 1

correlation (Scheme 1), or whether the presence of hydrogens at the first or second nitrogen atom may lead to the formation of other types of products. Consequently, this work was aimed at examining the gas-phase elimination kinetics of the hydrazo substituent H_2NNH at the acid side of esters such as ethyl and *tert*-butyl carbazates. Theoretical studies were also performed for an adequate interpretation of the mechanisms of these elimination reactions. The theoretical calculations aimed to procure the kinetic parameters and the characterization of the potential energy surface (PES) as a means to understand the nature of the molecular mechanism of these reactions.

COMPUTATIONAL METHOD AND MODEL

The kinetics of the gas-phase elimination reaction of ethyl and *tert*-butyl carbazates were studied using *ab initio* RHF, MP2 and DFT/B3LYP methods with 6-31G, 3-21G* and 6-31G* basis sets as implemented in Gaussian 98W.⁹ The Berny analytical gradient optimization routines were used for optimization. A transition states search was performed using the Quadratic Synchronous Transit protocol as implemented in Gaussian 98W. The nature of stationary points was established by calculating and diagonalizing the force constant matrix to determine the number of imaginary frequencies. Intrinsic reaction coordinate (IRC) calculations were performed to verify transition-state structures. The unique imaginary frequency associated with the transition vector (TV), i.e. the eigenvector associated with the unique negative eigenvalue of the force constant matrix, was characterized. Frequency calculations provided thermodynamic quantities such as zero point vibrational energy (ZPVE), temperature corrections and absolute entropies, and consequently the rate coefficient can be estimated assuming that the transmission coefficient is equal to 1. Temperature corrections and absolute entropies were obtained assuming ideal gas behavior from the harmonic frequencies and moments of inertia by standard methods¹⁰ at average temperature and pressure values within the experimental range. Scaling factors for frequencies and zero point energies for the HF, B3LYP and MP2 methods used were taken from the literature.¹¹

The first-order rate coefficient $k(T)$ was calculated using the TST¹² and assuming that the transmission coefficient is equal to 1, as expressed in the following relation:

$$k(T) = (KT/h)\exp(-\Delta G^\ddagger/RT)$$

where ΔG^\ddagger is the Gibbs free energy change between the reactant and the transition state and K and h are the Boltzman and Plank constants, respectively.

ΔG^\ddagger was calculated using the relations

$$\Delta G^\ddagger = \Delta H^\ddagger - T\Delta S^\ddagger$$

and

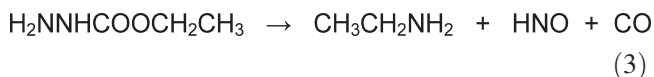
$$\Delta H^\ddagger = V^\ddagger + \Delta ZPVE + \Delta E(T) + PV$$

where V^\ddagger is the potential energy barrier and $\Delta ZPVE$ and $\Delta E(T)$ are the differences in ZPVE and temperature corrections between the transition state and the reactant, respectively.

RESULTS AND DISCUSSION

Ethyl carbazate

Complete kinetic studies of ethyl carbazate were difficult. However, the products of elimination of this substrate, in a vessel seasoned with allyl bromide and in the presence of toluene inhibitor, are predominantly ethylamine, HNO and CO, with traces amount of ethylene, hydrazine and CO₂. The stoichiometry based on the reaction (3)



has to give a ratio of 3.0 for P_f/P_0 , where P_f and P_0 are the final and initial pressures, respectively. Four measurements in the temperature range 310–340 °C with initial pressures around 60 Torr (1 Torr = 133.3 Pa) gave a mean value of 2.91. The reaction was found to be homogeneous in seasoned Pyrex vessels. However, some heterogeneous effect on the rate, in clean packed and unpacked Pyrex vessels, was obtained.

The effect of addition of different proportions of the free radical inhibitor toluene can be seen from Table 1. Nevertheless, the elimination reaction was carried out in the presence of at least twice the amount of the inhibitor in order to suppress any possible free radical chain processes. No induction period was observed. The rate coefficients were reproducible with a relative standard deviation not greater than 5% at a given temperature.

The first-order rate coefficients of ethyl carbazate, calculated from $k_1 = (2.303/t)\log[2P_0/(3P_0 - P_t)]$, was found to be invariable of the initial pressure (Table 2). A plot of $\log(3P_0 - P_t)$ against time t gave a good straight line up to 42% decomposition (Fig. 1). The variation of

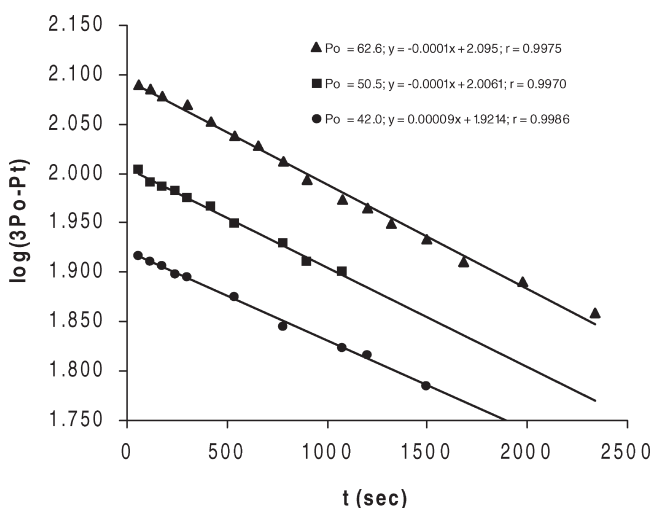
Table 1. Effect of free radical inhibitor toluene on rates

Substrate	Temperature (°C)	P_s (Torr) ^a	P_i (Torr) ^a	P_i/P_s	$10^4 k_1$ (s ⁻¹)
Ethyl carbazate	320.7	70	—	—	3.84
		65.5	33	0.5	2.41
		42	73.5	1.7	2.17
		62.5	116.5	1.9	2.18
		60	180.5	3.0	2.10
<i>tert</i> -Butyl carbazate	250.2	47	—	—	10.74
		41.9	58	1.4	10.66
		49.5	94	1.9	10.03
		40.8	108.5	2.7	10.69

^a P_s = pressure of the substrate; P_i = pressure of the inhibitor.

Table 2. Variation of rate coefficients with initial pressure

Substrate	Temperature (°C)	Parameter	Values			
Ethyl carbazate	320.7	P_0 (Torr)	42	50.5	62.5	
		$10^4 k_1$ (s ⁻¹)	2.27	2.10	2.18	
<i>tert</i> -Butyl carbazate	250.2	P_0 (Torr)	21.1	39.6	49.5	57.6
		$10^4 k_1$ (s ⁻¹)	9.93	10.74	10.66	10.76

**Figure 1.** $\log(3P_0 - P_t)$ vs time (t) for ethyl carbazate at 320.7°C

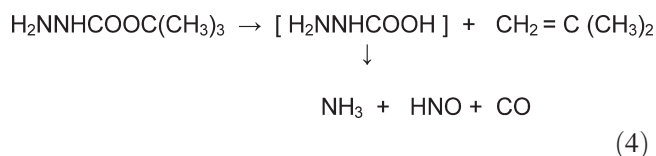
rate coefficients with temperature and the corresponding Arrhenius equation are given in Table 3 (90% confidence limits from a least-squares procedure).

Table 3. Variation of rate coefficients with temperature

Substrate	Parameter	Values				
Ethyl carbazate	Temperature (°C)	310.0	320.7	329.3	341.7	
	$10^4 k_1$ (s ⁻¹)	1.12	2.18	3.70	7.26	
Rate equation: $\log[k_1 \text{ (s}^{-1}\text{)}] = (11.84 \pm 0.22) - [(176.2 \pm 2.5) \text{ kJ mol}^{-1}] (2.303RT)^{-1}$; $r = 0.9998$						
<i>tert</i> -Butyl carbazate	Temperature (°C)	220.3	230.2	240.1	250.2	260.8
	$10^4 k_1$ (s ⁻¹)	1.18	2.51	5.22	10.18	20.23
Rate equation: $\log[k_1 \text{ (s}^{-1}\text{)}] = (12.34 \pm 0.29) - [(153.6 \pm 2.9) \text{ kJ mol}^{-1}] (2.303RT)^{-1}$; $r = 0.9999$						

tert-Butyl carbazate

The elimination products of *tert*-butyl carbazate in a vessel seasoned with allyl bromide are mainly isobutene, NH₃, HNO, and CO. The stoichiometry of the reaction



was checked by measurements of the ratio P_f/P_0 of final, to initial pressure. The average experimental result at four different temperatures (230–260°C) and 10 half-lives was 3.93. The theoretical stoichiometry of reaction (4) demands $P_f = 4P_0$. To check the stoichiometry of this elimination, the percentage decomposition obtained from pressure measurements was found to be in good agreement with the quantitative chromatographic analyses of isobutene formation (Table 4).

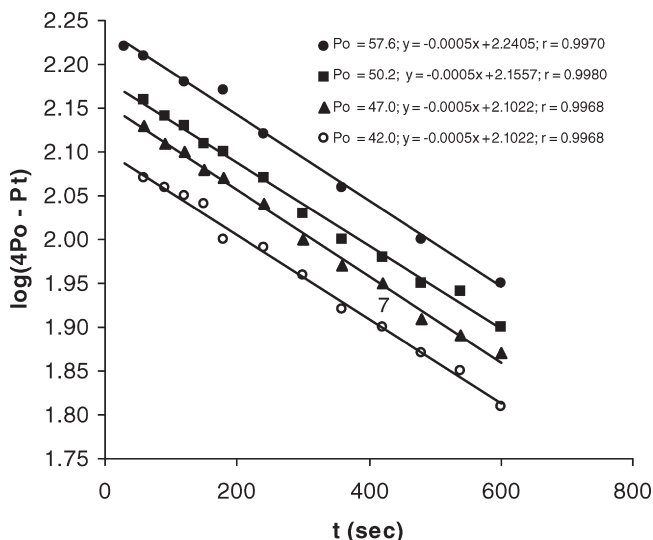
The homogeneity of reaction (4) was examined by using vessels with a surface-to-volume ratio of 6.0, greater than that of the unpacked vessels (1.0). The rates were unaffected in seasoned vessels, yet a small effect was found in clean packed and unpacked Pyrex vessels. The lack of a free-radical chain process in this reaction was examined by carrying out several runs in the presence of different proportions of the inhibitor toluene (Table 1).

The rates of pyrolysis elimination calculated from equation $k_1 = (2.303/t) \log[3P_0/(4P_0 - P_t)]$ and also be estimated from quantitative chromatographic analyses of isobutene formation using the equation $k_1 = (2.303/t) \log[P_0/(2P_0 - P_t)]$ are independent of the initial pressure of the carbazate, and the first-order plots of $\log(4P_0 - P_t)$ against time t are satisfactory up to 50% decomposition (Table 2, Fig. 2). The temperature dependence of the reaction and the corresponding Arrhenius equation are shown in Table 3. The rate coefficients are reproducible with a relative standard deviation not greater than 5% at a given temperature. The errors were estimated to 90% confidence limits from a least-squares procedure.

In order to use the results shown in Table 5 to provide reasonable mechanisms of elimination of ethyl and *tert*-butyl carbazates, a theoretical examination was undertaken.

Table 4. Stoichiometry of the reaction

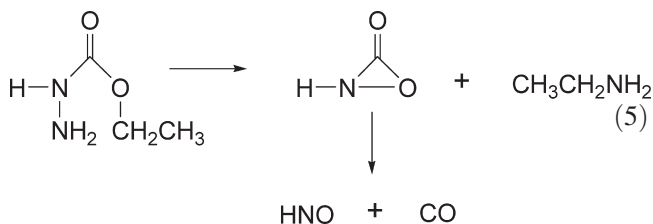
Substrate	Temperature (°C)	Parameter	Values				
<i>tert</i> -Butyl carbazate	250.2	Time (min)	4	6	8	10	12
		Reaction (%) (pressure)	21.9	31.1	38.1	44.9	50.1
		Isobutene (%) (GC)	21.1	29.7	40.7	46.7	51.7

**Figure 2.** $\log(4P_0 - P_t)$ vs time (t) for *tert*-butyl carbazate at 250.2 °C

THEORETICAL RESULTS

Ethyl carbazate

From the experimental observation that ethyl carbazate undergoes thermal decomposition to give ethylamine, HNO and CO, the theoretical studies on the mechanism of elimination of this ester were carried out based on the assumption that the reaction occurs in a two-step process. In a first rate-determining step, ethyl carbazate eliminates ethylamine and an unstable cyclic intermediate oxaziridinone COONH, which rapidly decomposes to give HNO and CO as shown in Eqn (5).

**Table 5.** Kinetic and thermodynamic parameters at 280 °C

Substrate	$10^4 k_1$ (s^{-1})	E_a (kJ mol^{-1})	$\log [A$ (s^{-1})]	ΔS^\ddagger ($\text{J mol}^{-1} \text{K}^{-1}$)	ΔH^\ddagger (kJ mol^{-1})	ΔG^\ddagger (kJ mol^{-1})
Ethyl carbazate	0.16	176.2 ± 2.5	11.84 ± 0.22	-31.6	171.6	189.1
<i>tert</i> -Butyl carbazate	68.0	153.6 ± 2.9	12.34 ± 0.29	-22.1	149.0	161.2

Geometries for the reactant, transition state (TS) and products for the rate-determining step were optimized using *ab initio* RHF, MP2 and DFT/B3LYP methods with 6-31G, 3-21G* and 6-31G* basis sets. Frequency calculations at the average experimental temperature and pressure (598.57 K and 0.09917 atm) were carried out.

Even though theoretical calculations of transition-state structures have been a useful tool for reasonable mechanistic interpretations of organic reactions, the results have usually been limited to enthalpy of activation, and consequently to energy of activation. Reasonable entropy values are rarely obtained directly from frequency calculations. This was the case for the thermal decomposition of ethyl carbazate. It is our experience in true gas-phase reactions that the difference in values between experimental energy of activation (E_a^{exp}) and the free energy of activation ($\Delta G^\ddagger_{\text{exp}}$) gives an idea of the magnitude of the entropy of activation.

In view of the above considerations, entropy values are estimated as follows. If

$$\Delta H^\ddagger_{\text{exp}} \approx \Delta H^\ddagger_{\text{theo}}$$

consequently

$$E_a^{\text{exp}} \approx E_a^{\text{theo}}$$

and therefore we expect that

$$\Delta G^\ddagger_{\text{exp}} \approx \Delta G^\ddagger_{\text{theo}}$$

We may define

$$\Delta G^\ddagger_{\text{exp}} - E_a^{\text{exp}} = C^{\text{exp}}$$

to obtain

$$\Delta G^\ddagger_{\text{theo}} = E_a^{\text{theo}} + C^{\text{exp}}$$

where the superscripts exp and theo refer to experimental and theoretical values, respectively, and the parameter C^{exp} is

$$C^{\text{exp}} = nRT - T\Delta S^\ddagger_{\text{exp}}$$

$n = 1$, unimolecular reaction.

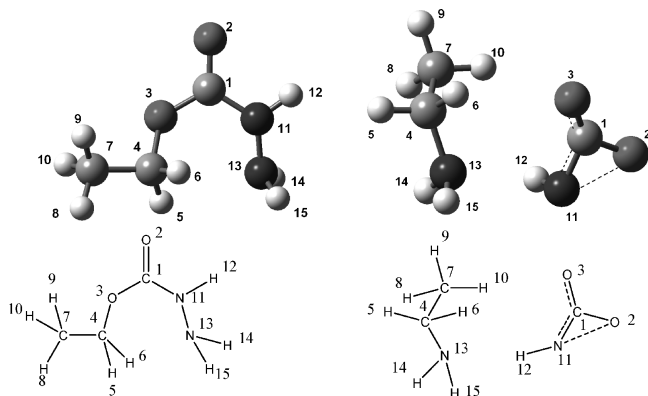


Figure 3. Thermal decomposition of ethyl carbazate (left) and TS structure (right) at 598.57 K and 0.09917 atm (B3LYP/6–31G). Schematic drawings with atom numbers are shown at the bottom

C^{exp} includes the contribution of collisional entropy, which has not been considered in frequency calculations (isolated molecules). Using

$$\Delta G^{\ddagger, \text{theo}} = \Delta H^{\ddagger, \text{theo}} - T\Delta S^{\ddagger, \text{theo}}$$

$\Delta S^{\ddagger, \text{theo}}$ was obtained. From $\Delta S^{\ddagger, \text{theo}}$ and E_a^{theo} , $\log A$ and the rate coefficients can be calculated.

Several low-energy conformations of the reactant were found. At the working temperature there is enough thermal energy for these conformations to interconvert [barriers ranging from 1.2 to 8.2 kcal mol⁻¹] (1 kcal = 4.184 kJ). The conformation shown in Fig. 3 is a local minimum showing an orientation close to the TS structure or reactive conformation.

Calculation results for the RHF, B3LYP and MP2 methods are given in Table 6. Rate coefficients and Arrhenius pre-exponential factors were determined and compared with the experimental values. The results show the best agreement for the B3LYP/6–31G method for all activation parameters (Table 6), within 2.2, 2.0, 1.9, 0.7% of error for ΔH^{\ddagger} , E_a , ΔG^{\ddagger} and ΔS^{\ddagger} , respectively. The first-order rate coefficient is of the same order of magnitude as the experimental value. The best calculated values were used to select the TS geometry for further analysis (Fig. 3).

Structural parameters for ethyl carbazate and for the TS at the B3LYP/6–31G level at 598.15 K and 0.09917 atm are given in Table 7. The TS configuration is a quasi-cyclic structure similar to the proposed intermediate oxaziridinone (atoms C1, O2 and N11 are positioned in a three-membered-like ring), where the O2—N11 distance is too large for a formal bond (1.77 Å in the TS) and C1—O2 has double bond character (1.216 Å). In the TS O3—C4 breaking is complete (3.57 Å in the TS) and substantial progress is also observed in N11—N13 bond breaking (2.59 Å in the TS). Analysis of NBO charges shows an increase in partial charge on C4 (from -0.068 to -0.253 in the TS, that is, C4 becomes more positive) and also on N13 (from -0.758 to -0.992 in the TS, i.e. N13 becomes more negative) and a decrease in the negative partial charge on N11 (from -0.605 to -0.366 in the TS), resulting in marked polarization of the O3—C4 and N11—N13 bonds in the TS.

Bond order analysis. To investigate further the nature of the TS along the reaction pathway, NBO bond order calculations were performed.^{13–15} Wiberg bond indexes¹⁶ were computed using the NBO program¹⁷ as implemented in Gaussian 98W. Bond breaking and making processes involved in the reaction mechanism can be monitored by means of the synchronicity (S_y) concept proposed by Moyano *et al.*,¹⁸ defined by the expression

$$S_y = 1 - \left[\frac{\sum_{i=1}^n |\delta B_i - \delta B_{\text{av}}| / \delta B_{\text{av}}}{2n - 2} \right]$$

where n is the number of bonds directly involved in the reaction and the relative variation of the bond index is obtained from

$$\delta B_i = [B_i^{\text{TS}} - B_i^{\text{R}}] / [B_i^{\text{P}} - B_i^{\text{R}}]$$

where the superscripts R, TS and P, represent reactant, transition state and product, respectively.

The evolution in bond change is calculated as

$$\%Ev = \delta B_i \times 100$$

Table 6. Ethyl carbazate activation parameters for the thermal decomposition at 325.0 °C and 0.09917 atm^a

Level of theory	ΔH^{\ddagger} (kJ mol ⁻¹)	E_a (kJ mol ⁻¹)	ΔG^{\ddagger} (kJ mol ⁻¹)	ΔS^{\ddagger} (J mol ⁻¹ K ⁻¹)	Log [A (s ⁻¹)]	$10^4 k_1$ (s ⁻¹)
RHF/6–31G	246.9	251.3	264.2	-28.9	12.02	1.06×10^{-6}
B3LYP/6–31G	174.9	179.8	192.7	-29.7	11.97	1.85
MP2/6–31G	150.9	155.9	168.8	-29.9	11.97	226.6
MP2/3–21G*	165.6	170.5	183.4	-29.7	11.97	12.02
MP2/6–31G*	163.8	168.8	181.7	-29.9	11.97	16.90
Experimental	171.6	176.2	189.1	-29.9	11.97	3.82

^a Free energy values were calculated using the parameter C^{exp} (12.9 kJ mol⁻¹). From these and ΔH^{\ddagger} from frequency calculations, entropy values were obtained.

Table 7. Structural parameters for ethyl carbazate and the TS for thermal decomposition at 598.57 K and 0.09917 atm (B3LYP/6-31G method) (atom distances in Å and dihedral angles in degrees)

Structure	C1—O3	O3—N11	O3—C4	N11—N13	C4—N13
Ethyl carbazate	1.373	2.370	1.480	1.390	2.890
TS	1.216	2.470	3.570	2.590	1.480
Product	1.380	1.710	3.510	2.710	1.490

	N11—C1—O3	O2—C1—O3	O2—C1—N11
Ethyl carbazate	118.41	120.91	120.67
TS	141.06	139.18	79.71
Product	76.61	137.72	144.97

Atomic charges from NBO analysis for ethyl carbazate and the TS for thermal decomposition (B3LYP/6-31G method):

Structure	C1	O2	O3	C4	N11	N13
Ethyl carbazate	1.090	-0.710	-0.666	-0.068	-0.605	-0.758
TS	1.018	-0.530	-0.633	-0.253	-0.367	-0.992

The average value is calculated from

$$\delta B_{\text{av}} = 1/n \sum_{i=1}^n \delta B_i$$

Bonds indexes were calculated for those bonds involved in the reaction changes, i.e. O3—N11 (B_{3-11}), O3—C4 (B_{3-4}), C4—N13 (B_{4-13}) and N11—N13 (B_{11-13}). The C1—O2 and C1—O3 bonds remain practically unaltered during the process.

NBO analysis results are given in Table 8. The synchronicity parameter $S_y = 0.731$ suggest a concerted non-synchronous mechanism, where the breaking of the O3—C4 bond plays an important role.

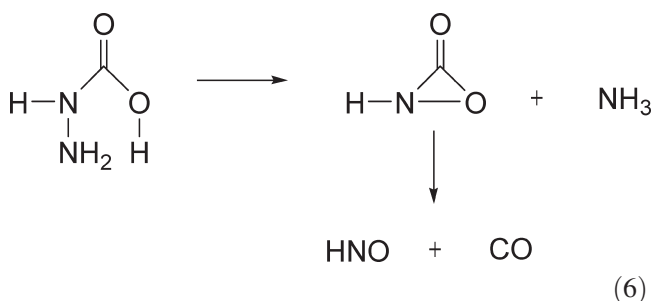
tert-Butyl carbazate

Theoretical studies on the mechanism of elimination of *tert*-butyl carbazate were based on the hypothesis that the reaction occurs in a two-step process, the first step giving isobutylene and H_2NNCOOH being rate determining, as shown in Eqn (4). Under the conditions of the reaction,

Table 8. NBO analysis for ethyl carbazate thermal decomposition at 598.57 K and 0.09917 atm (B3LYP/6-31G level): Wiberg bond indexes (B_i), % evolution through the reaction coordinate (%Ev), average bond index variation (δB_{av}) and synchronicity parameter (S_y)

Parameter	O3—N11	O3—C4	C4—N13	N11—N13
B_i^{R}	-0.0378	0.5707	-0.0010	0.9499
B_i^{TS}	-0.5440	-0.0003	0.7743	0.0194
B_i^{P}	0.6768	0.0006	0.7511	-0.2040
%Ev	70.83	100.15	103.08	19.36
δB_{av}		0.283		
S_y		0.731		

the intermediate NH_2NHCOOH proceeds to give NH_3 and the unstable oxaziridinone COONH is believed to decompose rapidly to HNO and CO gas [reaction (6)].



Geometries of the reactant *tert*-butyl carbazate and the intermediate products isobutylene and H_2NNCOOH were optimized using *ab initio* RHF, MP2 and DFT/B3LYP methods with 6-31G, 3-21G* and 6-31G* basis sets. Quadratic Synchronous Transit calculations were performed to obtain TS structures.

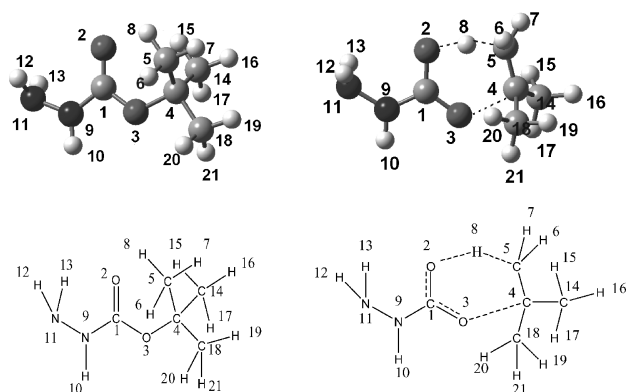
Frequency calculations at the average experimental temperature and pressure (513.45 K and 0.055197 atm) were carried out for the reactant *tert*-butyl carbazate, the TS and products of the rate-determining step. Calculation results for RHF, B3LYP and MP2 methods are given in Table 9. The best agreement in E_a and ΔH^\ddagger were found for both the MP2/6-31G and MP2/6-31G* levels of theory. Agreement with experimental values is within 2.4, 1.4, 1.4 and 5.0% error for ΔH^\ddagger , E_a , ΔG^\ddagger and ΔS^\ddagger , respectively. As for ethyl carbazate, entropies for *tert*-butyl carbazate were obtained using the C^{exp} parameter to estimate ΔG^\ddagger . The best calculated values were used to select the best TS geometry for further analysis (Fig. 4).

The TS structure for *tert*-butyl carbazate thermal decomposition is an almost planar six-membered ring where the hydrogen being transferred is half way between O2 and C5, and there is partial double bond character of

Table 9. *tert*-Butyl carbazate activation parameters for the thermal decomposition at 240.3 °C and 0.055197 atm^a

Level of theory	ΔH^\ddagger (kJ mol ⁻¹)	E_a (kJ mol ⁻¹)	ΔG^\ddagger (kJ mol ⁻¹)	ΔS^\ddagger (J mol ⁻¹ K ⁻¹)	Log [A (s ⁻¹)]	$10^4 k_1$ (s ⁻¹)
RHF/6-31G	142.2	146.0	153.6	-22.2	12.30	24.4
B3LYP/6-31G	115.7	120.0	127.6	-23.2	11.09	1120.0
MP2/6-31G	151.8	155.8	163.4	-22.6	12.28	2.55
MP2/3-21G*	170.6	174.6	182.2	-22.6	12.28	0.031
MP2/6-31G*	148.5	152.5	160.1	-22.6	12.28	5.52
Experimental	149.0	153.6	161.2	-23.8	12.22	4.27

^aFree energy values were calculated using the parameter C^{exp} (7.6 kJ mol⁻¹). From these and ΔH^\ddagger from frequency calculations, entropy values were obtained.

**Figure 4.** Thermal decomposition of *tert*-butyl carbazate (left) and TS structure (right) at 513.47 K and 0.055197 atm (MP2/6-31G). Schematic drawings with atom numbers are shown at the bottom

both the C1—O3 and C1—O2 bonds (Fig. 2). Structural parameters for *tert*-butyl carbazate and the TS are given in Table 10. In the TS structure there is substantial progress in O3—C4 bond breaking (2.17 Å) and O2—H8 bond formation (1.35 Å), an important double bond character of C1—O3 (1.30 Å) and intermediate progress in double bond formation for C4—C5 (1.42 Å). Analysis

of NBO charges shows an increase in partial charge on C4 (from 0.325 to 0.456 in the TS), an increase in partial charge on O3 (from -0.691 to -0.846 in the TS), an increase in partial charge on C5 (from -0.713 to -0.883 in the TS) and an increase in positive partial charge on H8 (from 0.270 to 0.469 in the TS), resulting in polarization of the O3—C4 and C4—C5 bonds in the TS. The bond angles show progress in hybridization change from sp^3 to sp^2 in C4; both C5—C4—C14 and C5—C4—C18 are close to 120° in the TS.

Bond order analysis. NBO bond order calculations were performed¹³⁻¹⁵ to investigate further the nature of the TS along the reaction pathway. Wiberg bond indexes¹⁶ were computed using the NBO program¹⁷ as implemented in Gaussian 98W. Synchronicity (S_y), δB_i , % E_v and δB_{av} values were determined as described above.

Bonds indexes were calculated for those bonds being modified during the reaction, i.e. C1—O2 (B_{1-2}), C1—O3 (B_{1-3}), O3—C4 (B_{3-4}), C4—C5 (B_{4-5}), C5—H8 (B_{5-8}) and O2—H8 (B_{2-8}). NBO results are given in Table 11. The greatest progress in the reaction coordinate is the breaking of the O3—C4 bond. The synchronicity parameter $S_y = 0.882$ and partial charges in the TS suggest a

Table 10. Structural parameters for *tert*-butyl carbazate and the TS for thermal decomposition at 513.47 K and 0.055197 atm (MP2/6-31G method) (atom distances in Å and dihedral angles in degrees)

Structures	C1—O2	C1—O3	O3—C4	C4—C5	C5—H8	O2—H8
<i>tert</i> -Butyl carbazate	1.258	1.390	1.520	1.537	1.090	2.450
TS	1.390	1.300	2.170	1.420	1.300	1.350
Product	1.520	1.250	3.470	1.354	2.310	0.980
	O2—C1—O3		C5—C4—C14		C5—C4—C18	
<i>tert</i> -Butyl carbazate	126.69		112.87		111.63	
TS	124.62		119.96		120.14	
Product	124.20		122.19		122.19	

Atomic charges from NBO analysis for *tert*-Butyl carbazate and the TS for thermal decomposition (MP2/6-31G method):

Structure	C1	O2	O3	C4	C5	H8	N9
<i>tert</i> -Butyl carbazate	1.075	-0.764	-0.691	0.325	-0.713	0.270	-0.588
TS	1.082	-0.859	-0.846	0.456	-0.883	0.469	-0.593

Table 11. NBO analysis for *tert*-butyl carbazate thermal decomposition at 513.45 K and 0.055197 atm (MP2/6–31G level): Wiberg bond indexes (B_i), % evolution through the reaction coordinate (% E_v), average bond index variation (δB_{av}) and synchronicity parameter (S_y)

Parameter	C1—O2	C1—O3	O3—C4	C4—C5	C5—H8	O2—H8
B_i^R	1.1810	0.6997	0.5362	0.9820	0.7229	0.0017
B_i^{TS}	0.8919	0.9881	0.1207	1.1986	0.3341	0.1576
B_i^P	0.701	1.1801	0.0001	1.8361	0.0155	0.4221
% E_v	60.23	60.03	77.50	25.36	54.96	
δB_{av}			0.568			
S_y			0.882			

concerted non-synchronous mechanism, where the polarization of O3—C4 is rate determining.

CONCLUSIONS

Ethyl carbazate

Theoretical calculations on ethyl carbazate thermal decomposition were based on the assumption that the reaction occurs in a two step-process [reaction (5)], involving an unstable three-membered ring intermediate, oxaziridinone. The TS structure obtained supports the mechanistic hypothesis and the formation of the intermediate oxaziridinone, because the TS found is similar to this intermediate as shown in Fig. 3. The results therefore suggest that the reaction proceeds by a concerted non-synchronous mechanism, through a quasi-three-membered ring transition state. Structural parameters, partial charges and NBO analysis suggest that polarization of O3—C4 bond is the determining factor in the decomposition process. The synchronicity parameter $S_y = 0.731$ is in accord with a concerted non-synchronous polar type of mechanism. Reasonable agreement of the activation parameters with the experimental parameters was found for the B3LYP/6–31G method.

tert-Butyl carbazate

Theoretical calculations suggest that the reaction proceeds via a concerted non-synchronous mechanism. The TS structure for *tert*-butyl carbazate thermal decomposition is an almost planar six-membered ring with the hydrogen being transferred located half way between O2 and C5. The activation parameters are in agreement with the experimental values for both the MP2/6–31G and MP2/6–31G* levels of theory and the first-order reaction rate coefficient of in the same order of magnitude.

Results from calculations and the agreement with experiment suggest the validity of the methods and mechanistic assumption proposed. Comparison of the

synchronicity parameters for ethyl and *tert*-butyl carbazate implies a more polarized asynchronous mechanism for ethyl carbazate ($S_y = 0.731$) compared with *tert*-butyl carbazate ($S_y = 0.882$).

With regard to the methods used, ethyl carbazate gave the best results with the B3LYP/6–31G method whereas for *tert*-butyl carbazate the best parameters were obtained with both the MP2/6–31G and MP2/6–31G* methods. For ethyl carbazate, the electronic distribution in the TS structure is more polarized and there is more charge separation. For this molecular system, a different level of electron correlation energy may be involved. The MP4 perturbation method accounts for ~95% of electron correlation energy or more, compared with multilevel correlated methods such as CC and CI theories. MP2, being a lower level of calculation, does not account for the total correlation energy. In this case DFT methods using hybrid ACM functionals such as B3LYP give better results.

For the thermal decomposition of *tert*-butyl carbazate, entropy values were obtained directly from frequency calculations whereas for ethyl carbazate decomposition, entropy values were estimated using the empirical parameter C^{exp} described above.

EXPERIMENTAL

Ethyl carbazate (Aldrich) after several distillations and *tert*-butyl carbazate (Aldrich) both, with >99.0% purity [GC/MS (Saturn 2000, Varian), DB-5MS capillary column, 30 m \times 0.250 mm i.d., 0.25 μ m film thickness] were used. The product isobutene was quantitatively analyzed in a column of Porapak Q (80–100 mesh). The $CH_3CH_2NH_2$ product, when collected from the reaction vessel in the trap, reacts with the HNO to form a solid, $CH_3CH_2NH_3^+ NO^-$. This salt was identified by mass spectrometry. The free amine was obtained through a column of soda lime.

Kinetics

Kinetic studies were carried out in a static system as described previously^{19–21} with an Omega DP41-TC/DP41-RTD high-performance digital temperature indicator. The rate coefficients were calculated from pressure increase and from chromatographic analyses. The temperature was controlled by a resistance thermometer controller and an Omega Model SSR280A45 solid-state relay, maintained within $\pm 0.2^\circ C$ and measured with a calibrated platinum–platinum–13% rhodium thermocouple. No temperature gradient was detected along the reaction vessel. Both carbazate esters were dissolved in dioxane and injected directly into the reaction vessel with a syringe through a silicone rubber septum. The amount of substrates used for each run was ~0.05–0.1 ml.

REFERENCES

1. Herize A, Domínguez RM, Rotinov A, Nuñez O, Chuchani G. *J. Phys. Org. Chem.* 1999; **12**: 201–206.
2. Daly NJ, Ziolkowski F. *Aust. J. Chem.* 1972; **25**: 1453–1458.
3. Kwart H, Slutsky J. *J. Chem. Soc., Chem. Commun.* 1972; 552–553.
4. Kwart H, Slutsky J. *J. Chem. Soc., Chem. Commun.* 1972; 1182–1183.
5. Daly NJ, Ziolkowski F. *J. Chem. Soc., Chem. Commun.* 1972; 911–912.
6. Luiggi M, Dominguez RM, Rotinov A, Herize A, Cordova M, Chuchani G. *Int. J. Chem. Kinet.* 2002; **34**: 1–5.
7. Chuchani G, Nuñez O, Marcano N, Napolitano S, Rodríguez H, Domínguez M, Ascanio J, Rotinov A, Domínguez RM, Herize A. *J. Phys. Org. Chem.* 2001; **14**: 146–158.
8. Chuchani G, Domínguez RM, Rotinov A, Herize A. *J. Phys. Org. Chem.* 1999; **16**: 40–46.
9. Frisch MJ, Trucks GW, Schlegel HB, Scuseria GE, Robb MA, Cheeseman JR, Zakrzewski VG, Montgomery JA Jr, Stratmann RE, Burant JC, Dapprich S, Millam JM, Daniels AD, Kudin KN, Strain MC, Farkas O, Tomasi J, Barone V, Cossi M, Cammi R, Mennucci B, Pomelli C, Adamo C, Clifford S, Ochterski J, Petersson GA, Ayala PY, Cui Q, Morokuma K, Malick DK, Rabuck AD, Raghavachari K, Foresman JB, Cioslowski J, Ortiz JV, Stefanov BB, Liu G, Liashenko A, Piskorz P, Komaromi I, Gomperts R, Martin RL, Fox DJ, Keith T, Al-Laham MA, Peng CY, Nanayakkara A, Gonzalez C, Challacombe M, Gill PMW, Johnson B, Chen W, Wong MW, Andres JL, Gonzalez C, Head-Gordon M, Replogle ES, Pople JA. *Gaussian 98, Revision A.3.* Gaussian: Pittsburgh, PA, 1998.
10. McQuarrie D. *Statistical Mechanics.* Harper and Row: New York, 1986.
11. Foresman JB, Frish Æ. *Exploring Chemistry with Electronic Methods* (2nd edn). Gaussian: Pittsburgh, PA, 1996.
12. Benson SW. *The Foundations of Chemical Kinetics.* McGraw-Hill: New York, 1960.
13. Lendvay G. *J. Phys. Chem.* 1989; **93**: 4422–4429.
14. Reed AE, Weinstock RB, Weinhold F. *J. Chem. Phys.* 1985; **83**: 735–746.
15. Reed AE, Curtiss LA, Weinhold F. *Chem. Rev.* 1988; **88**: 899–926.
16. Wiberg KB. *Tetrahedron* 1968; **24**: 1083–1095.
17. *Gaussian NBO Version 3.1.* Gaussian: Pittsburgh, PA, 1998.
18. Moyano A, Periclas MA, Valenti E. *J. Org. Chem.* 1989; **54**: 573–582.
19. Maccoll A. *J. Chem. Soc.* 1955; 965–973.
20. Swinbourne ES. *Aust. J. Chem.* 1958; **11**: 314–330.
21. Dominguez RM, Herize A, Rotinov A, Alvarez-Aular A, Visbal G, Chuchani G. *J. Phys. Org. Chem.* 2004; **17**: 399–408.